

CLIMATE VARIABILITY OVER SUBTROPICAL SOUTH AMERICA AND THE SOUTH AMERICAN MONSOON: A REVIEW

Vicente Barros^{1,2}, Moira Doyle¹, Marcela González¹, Inés Camilloni^{1,3},
Rubén Bejarán¹ and Rubén M. Caffera⁴

¹ Department of Atmospheric and Oceanic Sciences. University of Buenos Aires, Argentina
² Consejo Nacional de Investigaciones Científicas y Tecnológicas (CONICET). Buenos Aires, Argentina
³ Centro de Investigaciones del Mar y la Atmósfera (CIMA)/ (CONICET). Buenos Aires, Argentina
⁴ University of La República. Montevideo, Uruguay

(Manuscript: received 10 July 2002; in final version: 20 December 2002)

RESUMEN

Este trabajo hace una revisión del Sistema del Monzón de América del Sur (SMAS) y sus relaciones con el clima de la región subtropical al sur de 20°S, basado en trabajos de los coautores y otras contribuciones. Se discuten los dos patrones dominantes de la circulación de capas bajas durante Enero y su asociación con las fases de alternancia en intensidad de la zona de convergencia del Atlántico Sur (ZCAS), el jet de capas bajas y el campo de precipitación al sur de 20°S. Estos patrones de circulación y los campos asociados de precipitación son consistentes con los indicadores del origen de las aguas meteóricas derivados de sus contenidos isotópicos. Cada uno de estos dos patrones de circulación y precipitación están asociadas a anomalías de la temperatura del mar en el oeste de la región subtropical del Atlántico Sur. Se examinan además algunas consecuencias del comportamiento del SMAS sobre las crecidas de los ríos Uruguay y Paraná. Las mayores crecidas del primero están precedidas de un flujo de capas bajas del noroeste con intensa advección cálida y húmeda. Las mayores crecidas del Paraná comienzan en la cuenca del Paraná medio y están asociadas a El Niño.

Palabras claves: monzón sudamericano, precipitación, caudales, temperatura de la superficie del mar

ABSTRACT

This paper reviews the relation of the South American Monsoon System (SAMS) with the climate of South America (SA) south of 20°S based on work of the coauthors and other contributions. Two dominant patterns of the midsummer low-level circulation are linked to the seesaw phases of the South Atlantic convergence zone (SACZ), the low-level jet and precipitation field. These circulation patterns and the associated precipitation are consistent with water sources indicators derived from the isotopic content of the meteoric water. Each of these circulation and precipitation patterns are associated with SST anomalies in the subtropical western South Atlantic. The influence of the SAMS on the discharges of the Uruguay and Paraná rivers is examined. The greatest discharges in the Uruguay River are preceded by strong humid, warm air advection. The highest discharge peaks in the Paraná River begin in the middle Paraná basin and are associated with remote patterns of low-frequency variability such as El Niño.

² First author's e-mail address: barros@at.fcen.uba.ar

Key words: monsoon, precipitation, river discharge, sea surface temperature.

1. INTRODUCTION

In the last years, it was devoted considerable attention to the South American Monsoon System (SAMS). However, most of the recent literature treats SAMS' features that are predominantly north of, or about 20°S. The relation of the SAMS with the climate of South America (SA) south of this latitude, which will be referred to as subtropical South America (SSA), has received less attention.

During the first stage of the SAMS, characterized by Zhou and Lau (1998) as the pre-monsoon phase, the low-level flow typical of the summer circulation is already present. It is a quasi-stationary easterly flow from the equatorial Atlantic Ocean that, when reaching the proximity of the Andes, turns south towards the subtropical region. This feature is present in all the analyses, independently of data sets (Zhou and Lau 1998). During September, the convective activity moves rapidly from the northwest of the Amazon basin towards the south and southeast, progressing later to the east (Kousky 1988; Marengo et al. 2001). This progress accompanies the establishment of a high at upper levels (Marengo, 1992; Rao et al., 1996). The upper level high shifts southwards, until it becomes established over the Bolivian plateau in the mature phase of the monsoon (Zhou and Lau 1998). The low-level flow from the tropics to the subtropical region and the Bolivian high are features -not the only ones- which reveal the links of the SAMS with the subtropical circulation. Some of these links are:

i) A frequent feature of the tropical convection during summer months in SA is its elongation towards the Atlantic Ocean at about 20°S. This prominent feature, known as the South Atlantic convergence zone (SACZ) (Kodama 1992), has a seesaw behavior in its intensity with an approximate duration of 8 days in each extreme phase (Nogués-Paegle and Mo 1997). Events with strong (weak) convective activity over the SACZ are associated with negative (positive) rainfall anomalies in the subtropical region south of the SACZ, and with a change in the low-level circulation from the tropics. In fact, the low-level winds are directed eastward (southeastward) at about 20°S in the case of strong (weak) SACZ events, together with an eastward (westward) shift

of the South Atlantic subtropical high (Nogués-Paegle and Mo 1997). A compensatory subsidence over northern Argentina and southern Brazil during the active phases of the SACZ was found through numerical experiments performed with an idealized tropical heat source that takes into account an additional heat source at the SACZ (Gandú and Silva Dias 1998). These numerical experiments also showed a southward shift of the Bolivian high (BH) during the active phase of the SACZ (Gandú and Silva Dias 1998).

ii) The main contribution to the precipitation minus evaporation budget in summer over SSA comes from the convergence of the mean water vapor transport (Labraga et al. 2000). Figure 1 shows the mean low-level circulation at 925 hPa, obtained from the NCEP/NCAR reanalysis. In July, there is a southward flow originating in the westward flow between 10°S and 20°S that turns southeastward south of 30°S. This flow determines a similar mean field of moisture flux (Doyle and Barros 2002) and it is roughly associated with the axis of maximum precipitation along its path (Fig. 1a). In January, the low-level flow from the tropical continent has a southeasterly direction converging with the southwestward winds of the South Atlantic high in the vicinity of the SACZ, at about 20°S (Fig. 1c). This flow turns to the south following an anticyclonic circulation over subtropical Argentina. The convergence of the mean low-level water transport in the continental extension of the SACZ over the continent is accompanied with a spatial maximum in precipitation, with values well above of 200 mm (Fig. 1c). In subtropical Argentina, the mean flow reaches the Andes, and in contrast to what occurs in winter, the region west of 60°W has considerable precipitation. The transition seasons represented by October and April have fairly similar fields, both in the low-level flow and in precipitation (Fig. 1b and 1d), although in October these fields resemble the respective January fields rather than those of July, and vice-versa in April. In general, there is a fair agreement between the low-level flow and the integrated water vapor transport calculated by Doyle and Barros (2002). Although the contribution of the transient components of the water vapor convergence to the monthly precipitation are important (Labraga et al. 2000),

Climate variability over Subtropical . . .

there is however, a good agreement between the east-west seasonal shift of the mean low-level flow

and the rainfall annual cycle in western Argentina (Fig. 1).

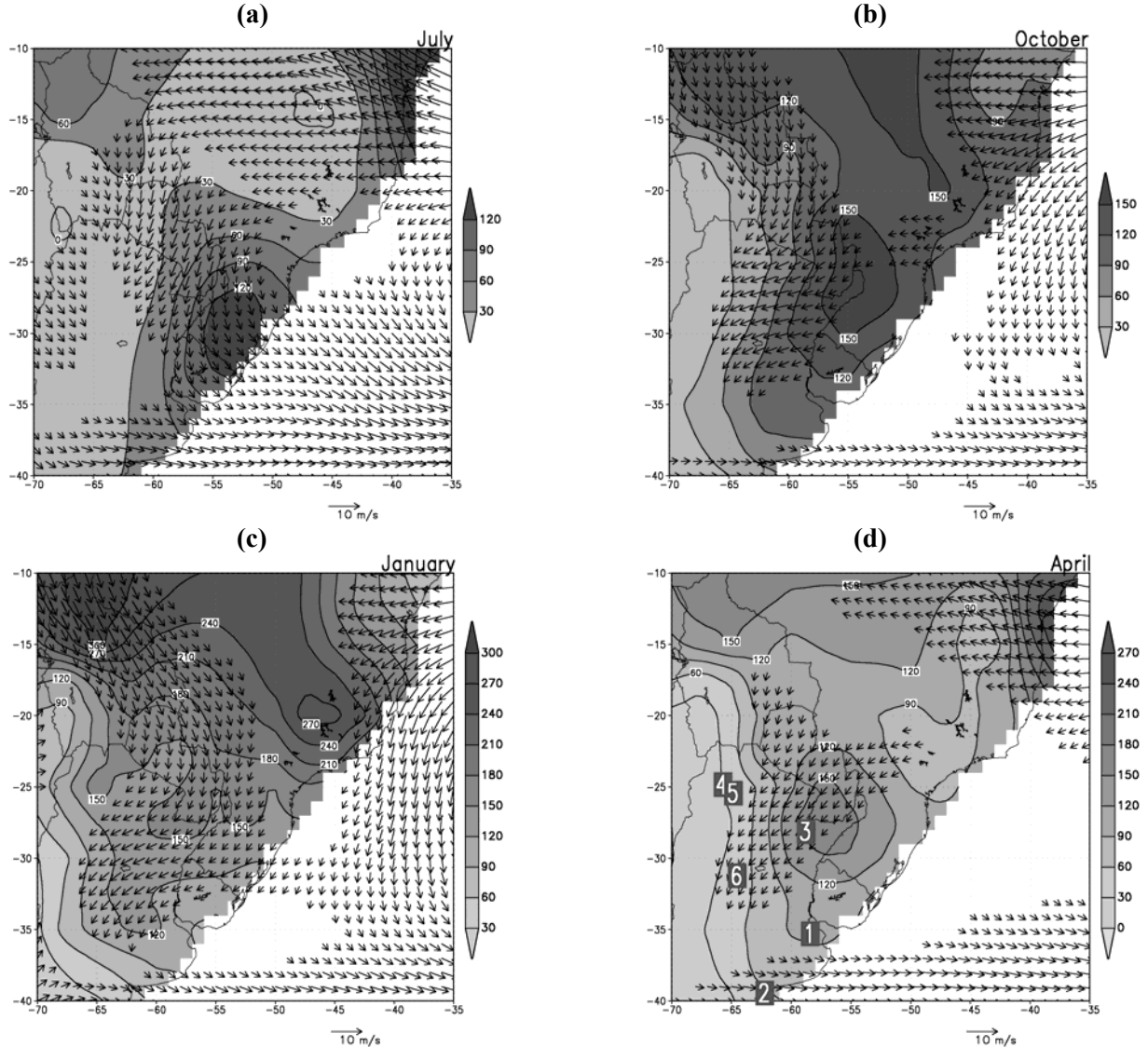


Figure 1: Mean (1958-1992) wind at 925hPa (intensity stronger than 2.5m/s shown) and mean (1956-1991) precipitation fields for (a) July, (b) October, (c) January and (d) April. Numbers in panel (d) indicate GNIP stations (See text in section 3.2) as follows: (1) Buenos Aires, (2) Bahia Blanca, (3) Corrientes, (4) Jujuy, (5) Salta and (6) Córdoba.

iii) There are observational evidences of a low-level jet (LLJ) embedded in the low-level southward flow, east of the Andes (Virji 1981; Paegle 1998). Numerical modeling evidence has been more frequent (see Berbery and Collini 2000, and references therein). Unlike the Great Plains LLJ, which is a warm-season phenomenon, the South American LLJ is present throughout the year, although in wintertime it has a somewhat different structure, with the core located at a higher elevation (Berbery and Barros 2002). The

mesoscale features of the LLJ cannot be well resolved by global reanalyses (Berbery and Rasmusson 1999; Berbery and Collini 2000), and therefore, the moisture advection that the southward low-level flow actually carries could be much higher than that calculated from these reanalyses.

iv) As a result of the advection of moisture from the tropical continent, enhanced by the presence of the LLJ throughout the year, and because of synoptic disturbances, the rainfall regime in eastern

SA south of 20°S has not a pronounced annual cycle. During the warm season (Oct-Apr), mesoscale convective complexes are frequent, and they account for a large part of the total precipitation (Velasco and Fritsch, 1987; Laing and Fritsch 2000). In addition, there are frequent cyclogenesis during the transition seasons over eastern SSA (Rao et al. 1996). During the cold season, the most relevant forcing is due to synoptic activity, which accounts for much of the seasonal precipitation in southeastern SA (Vera et al. 2002). On the other hand, in western Argentina and in the Chaco region stretching over Paraguay and Argentina, the rainfall regime has typical monsoon features. The rainy season begins in September, ending the dry winter season, and it lasts until the austral autumn (González and Barros 1998). This simultaneity with the solar cycle led some authors to consider this cycle as a typical feature of a continental regime (Prohaska 1976). However, as it can be seen from figure 1, there are indications that this seasonal variability of rainfall in those regions is also linked to the low-level flow variability from the tropical sources of humidity.

At this point, it is clear that the climate south of 20°S is connected with the tropical atmosphere. Thus, the objective of this paper is to review the relation of the SAMS with the low-level circulation, precipitation and surface temperature south of 20°S, both in midsummer and at the onset and end of the tropical convection. In addition, it is examined how these aspects are related to the discharge of the main rivers of La Plata Basin. The review of these issues is based upon results obtained by the co-authors and other authors. Following these lines, the paper is structured in seven sections. Section 2 describes data sets. Section 3 reviews the connection between the SACZ, the LLJ, low-level circulation and precipitation in SSA east of the Andes. The links between South Atlantic SST and the SACZ, the low-level circulation and precipitation are presented in Section 4. Section 5 addresses the link between the onset and end of the SAMS with the precipitation east of the Andes. Interannual variability of the hydrology of the most important rivers is examined in section 6. Finally, section 7 is a summary of the main aspects.

2. DATA

Monthly precipitation series (1956-1991) from stations located between 22°S and 40°S, east of the Andes were gathered from different sources. The Argentine National Meteorological Service and the National Direction of Meteorology of Paraguay provided the records for Argentina and Paraguay, respectively. Most of the series for Brazil were obtained from the Institute of Agricultural Research of Rio Grande do Sul and from the National Agency of Electricity. Data from Uruguay, Bolivia and additional series from Brazil were taken from the Monthly Climatic Data for the World files of the National Center for Atmospheric Research (NCAR). In this set of 117 monthly records, there are less than 2% missing data, and none of the series has more than 10% of absent data. Except in figure 8, monthly totals were averaged on a three-degree latitude by three-degree longitude array, in order to smooth the singularities of single raingauge measurements. Only for figure 2, because of the unavailability of daily data in most of SSA, daily precipitation was taken from the NCEP/NCAR daily reanalysis and its limitations are discussed in section 3 when this figure is presented.

Isotopic contents of meteoric water were taken from the Argentine stations of the Global Network for Isotopes in Precipitation (GNIP), which has collected rainfall samples all over the world since 1961. These stations took monthly rainfall samples to determine tritium, deuterium and oxygen-18 contents. Most of the Argentine stations have discontinuous records and are no longer operative. However, six stations collected data corresponding to more than 5 years, and their spatial distribution was such, that adequately represents the different rainfall regimes of subtropical Argentina (Fig. 1d).

OLR measurements from polar satellites of the National and Oceanographic Administration (NOAA), averaged on a 2.5° latitude-longitude array, were taken from the Climate Diagnostic Center (CDC) of the NOAA. The daily value was considered missing when either the day or the night data were not available. Missing values were recovered by spatial interpolation, except for 1978, when data were not available for most of the year.

Low-level winds from surface to 700 hPa, specific humidity and omega vertical velocity at 500 hPa were taken from the NCEP/NCAR reanalysis (Kalnay et al. 1996). Atlantic SST data from 10°N to 40°S, and from the South American

coast to 20°E were obtained from the Comprehensive Ocean - Atmosphere Data Set (COADS) (Woodruff et al. 1987).

Water vapor transport was calculated using the specific humidity (q) and wind (V) every six hours. As in many other regions, most of the water vapor in South America is concentrated in the low levels of the troposphere (Berbery and Collini 2000). Therefore, the water vapor transport (qV) was integrated from surface to 700 hPa using winds and specific humidity from the 1000, 925, 850 and 700 hPa levels. These values were calculated every six hours, and then averaged for each day. They were compared with the precipitable water column integrated up to 700 hPa derived from satellite and radiosonde observations in the NASA Water Vapor Project (NVAP) (Randel et al. 1996) for the 1988-1992 period (Doyle 2001). Over eastern SSA, the January - the month reported here- averages from NVAP and those calculated by Doyle (2001) differ in less than 2 mm, except in small areas and in the proximity of the Andes west of 65°W, where both data sets differ considerably. The relative difference in most of the region is considerably less than 10% and daily map correlation averages 0.87.

3. SACZ, THE LLJ AND THE LOW-LEVEL CIRCULATION AND PRECIPITATION SOUTH OF 20°S

3.1 Low-level water transport and precipitation

A Principal Component Analysis (PCA) of the water vapor transport (integrated from surface to 700 hPa) anomaly fields of January days (1958 to 1992) was performed. The first component explains 21% of the variance. Figure 2 presents the composites of the daily cases corresponding to the highly positive and highly negative values of the loading factor of the first principal component. Here, highly positive (negative) values are considered those above (below) the mean plus (minus) the standard deviation. The positive (negative) composite results from averaging 212 (220) days. The cases with sequences of highly positive (negative) values of the first factor loading are 94 (101). This means that each sequence lasts in the average little more than two days. This is so, because only extreme values are considered, while the events associated to each composite could last much longer. Hereinafter, these composites will be referred to as positive and negative composites.

In the positive composite, water vapor is transported by the trade-wind circulation at equatorial latitudes, which turns southeastward near the Andes towards eastern Argentina, southern Brazil and Uruguay. Part of this transport, east of the Andes, diverts southward over western subtropical Argentina. At about 20°S, the westward transport from the Atlantic Ocean merges with the southeastward transport. The composite of the precipitation field shows a maximum band along the east of the continent, with a maximum over southern Brazil and northeastern Argentina that is fed by the low-level convergence of the mean water transport (Fig. 2a). Another area of heavy precipitation is found east of the Andes. However, these precipitation fields should be considered with caution, since the precipitation composite is made up of daily rainfall calculated from the reanalysis, and thus, only the broad features of the fields deserve credit. When the mean January precipitation field (Fig. 1c) is compared with this composite, it is clear that this case corresponds to the weak SACZ phase. In fact, the heaviest precipitation in eastern SA is at about 30°S, while relatively less precipitation is accumulated in the area of the continental extension of the SACZ.

The positive composite includes the cases of the Chaco Jet Events (CJEs) as defined by Nicolini and Saulo (2000). They defined as CJEs, those cases when the LLJ penetrates southward of 25°S. A statistical analysis of these cases, using 15-year reanalysis of the European Centre for Medium Weather Range, indicates that the LLJ is present in 28% of the spring days, and in 17% of the summer days (Salio et al. 2002). The summer composite field of the vertically integrated moisture transport of the CJEs is basically similar to figure 2a and the spring composite is also qualitatively analogous (Salio et al. 2002). Regarding precipitation, the CJEs account for an important fraction of the seasonal precipitation in northeastern Argentina, northern Uruguay, eastern Paraguay and southern Brazil, reaching up to a maximum of 70% in spring and 55% in summer in some areas (Salio et al. 2002).

The basic structure of the water vapor transport in tropical latitudes in the negative composite (Fig. 2b) is elsewhere similar to that of the positive case, except that the main branch of the transport turns eastward towards the SACZ at about 20°S. In addition, the incoming flow from the Atlantic

Ocean converges with the flow from the western branch over eastern Brazil, increasing the convergence over the SACZ. The heavy precipitation over the SACZ and its continental extension is consistent with this circulation. South of 20°S there is an anticyclonic circulation that reflects the synoptic situations when the southwestern part of the South Atlantic high extends westward over Argentina, or a post-frontal

anticyclone is centered over subtropical Argentina (Fig. 2b). In these situations, the wind blows from the ocean over a considerable part of the eastern subtropical continent, exhibiting features of a giant sea-land breeze. Again, as in the positive case, the precipitation field indicates a clear association with one of the SACZ phases, in this case with the strong one.

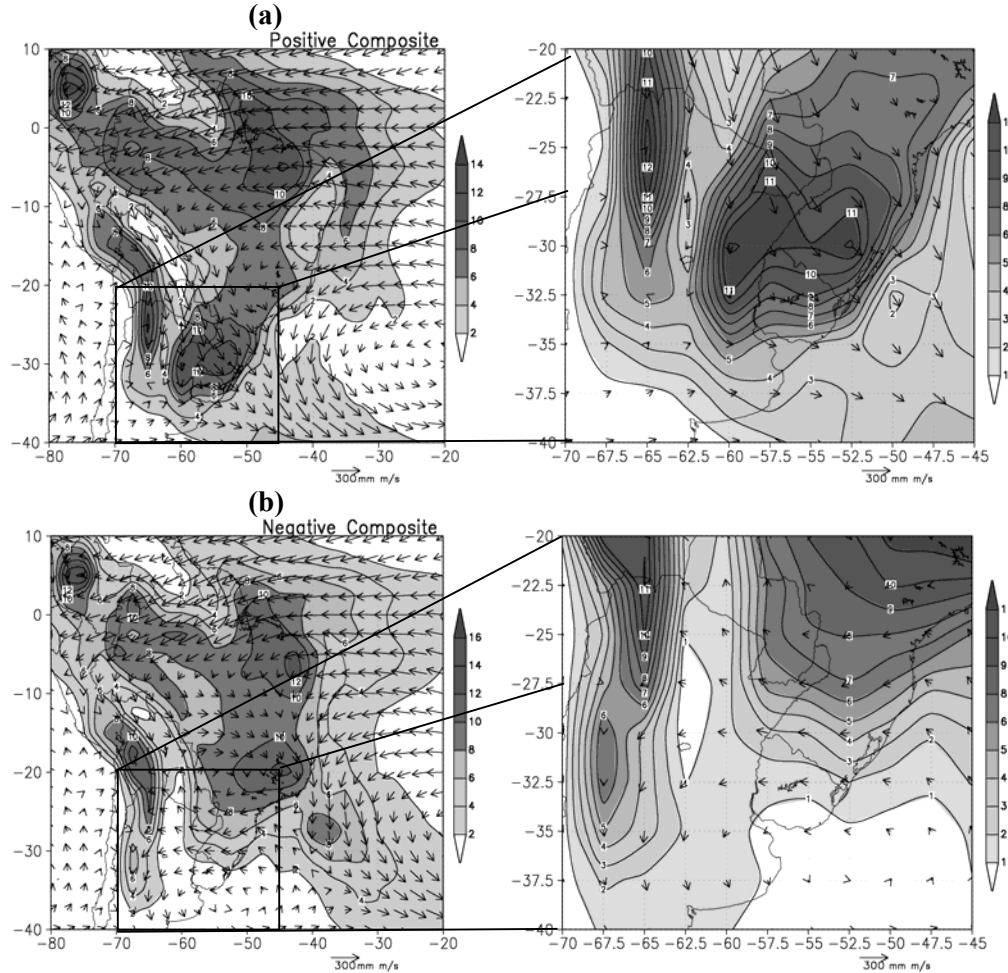


Figure 2: Composite of daily (January) water vapor transport and precipitation for (a) highly positive and (b) highly negative loading factors of the first principal component of the daily water vapor transport. Period 1958-1992. The right side panels present a detailed view of the area $20 - 40^{\circ}\text{S}$; $45 - 70^{\circ}\text{W}$. See text for the definition of highly positive and highly negative values.

North of 20°S , the moisture transport associated to weak and strong SACZ events calculated by Nogués-Paegle and Mo (1997) is practically the same as the one shown here (their figures 7 and 8). Moreover, the dipolar structure in the precipitation field is similar to the one described by Nogués-Paegle and Mo (1997), although they reach their results by composing fields that correspond to a

SACZ mode in the OLR field. In addition, enhanced (diminished) SACZ precipitation is accompanied by enhanced (reduced) precipitation in western Argentina, south of 30°S (Figs. 1 and 2). This feature cannot be attributed to pitfalls in the reanalysis data because it also appears in monthly composites of observed precipitation calculated according to the Atlantic Ocean SST (section 4),

which are accompanied by a low-level circulation field similar to that of the water vapor transport depicted in figure 2b. In addition, this is consistent with the fact that the westward wind component, not only transports water vapor from the Atlantic Ocean, but also favors the upward motion and the precipitation processes on the steeped slopes of the mountain chains to the east of the Andes (Figs. 2a and 2b).

The occurrence of the extreme positive or negative events of the first factor loading seems unrelated to the El Niño phase. In the sample of 35 months of January considered, 37% of them were El Niño months and the respective frequency of extreme positive (negative) events of the first factor loading corresponding to El Niño months was 40% (35%). On the other hand, some relation with La Niña months cannot be discarded. Its respective month frequency was 23%, while that of the extreme positive (negative) events of the first factor loading corresponding to La Niña months was 28% (18%).

3.2 Sources of the meteoric water

The Andes Mountains act as a barrier to the low-level access of moisture from the Pacific in the eastern side of the continent. Therefore, the only external sources of water vapor for rainfall in southeastern SA are the Atlantic Ocean and the tropical continent. The standard deviation of the water vapor transport in summer over most of eastern Argentina, Uruguay and southern Brazil is considerably greater than the mean flow (Doyle 2001). Therefore, the origin of the meteoric water cannot be truly estimated from the mean flow. A possible alternative to discriminate the origin of water that precipitates in a region is to analyze its isotopic content. (Schotterer et al. 1996; Rozanski et al. 1993). The basis for this kind of method is that the isotopic contents are related to the trajectory of the air mass because when the humid air moves from the ocean to a continental region, it is progressively depleted of isotopes as precipitable water is lost on the way.

The relation between oxygen-18 and deuterium in meteoric waters has been used to determine its maritime or continental origin. The best fit for all GNIP data is:

$$\text{DEU} = 8 * \text{O18} + 10 \quad (1)$$

where DEU is the deuterium content and O18 is the oxygen-18 content. Therefore, the deuterium excess (d_8) is defined as:

$$d_8 = \text{DEU} - 8 * \text{O18} \quad (2)$$

This last magnitude has been used to identify water vapor source regions. Higher d_8 is generally associated with re-evaporated moisture from continental areas. Therefore, deuterium excess and oxygen-18 content are potentially useful to distinguish the origin of meteoric water. In fact, in SA, Salati et al. (1978) found evidence of water recycling in the Amazon basin using isotopic concentrations in rainfall water.

In the case of the Argentine GNIP stations, the probable range for deuterium excess and oxygen-18 content that corresponds to the tropical continental water vapor source (C) or the Atlantic water vapor source (A) was estimated from the few cases that permitted the identification of their origin. The isotope content was only available from monthly-accumulated meteoric water. Therefore, in most of the cases it was impossible to determine a unique source, since the water could have been originated at different rainfall episodes with different water vapor origin. Only in about 50 out of 372 monthly-accumulated precipitation samples with measured contents of oxygen-18 and deuterium at any of the six GNIP stations was it possible to discern the source origin. Those were cases with only one rainfall episode in the month or eventually two cases with the same water vapor origin, namely the Atlantic or the tropical continent. In each of these cases, the winds at 850-hPa from the NCEP/NCAR reanalyses (Kalnay et al. 1996) were used to infer the trajectory of the air for a period of at least five days. These trajectories were calculated using hourly winds linearly interpolated from the wind fields of reanalysis, available every 6 hours. Trajectories were calculated using the GRADS program *Traj.gs* provided by Codina (<ftp://grads.iges.org/grads/scripts>). No attempt was made to calculate a 3-dimensional trajectory because with the available data it would have been impossible to estimate the height and thickness of the precipitating cloud. Thus, it was assumed that most of the water vapor entered the cloud at low levels. Trajectories using 925 hPa winds did not change the source origin of the cases that were retained for the subsequent analysis, namely those with a clear origin either in the

tropical continent or in the Atlantic. These cases amounted to only 21 due to the requirement that all of the monthly rainfall at the GNIP station should have the same source (Tropical SA or Atlantic Ocean).

Figure 3a shows the 21 classified cases in a d8-O18 diagram. In general, the continental cases have lower O18 and greater d8, as expected from theory. Out of the twelve cases classified as Atlantic Ocean (A), eleven fall into the A sector as defined by a discriminant analysis. Similarly, six out of the nine cases classified as Tropical Continental (C) fall in the C region. The Wilk's Lambda coefficient was 0.48 (0 indicates perfect and 1 indicates no discrimination).

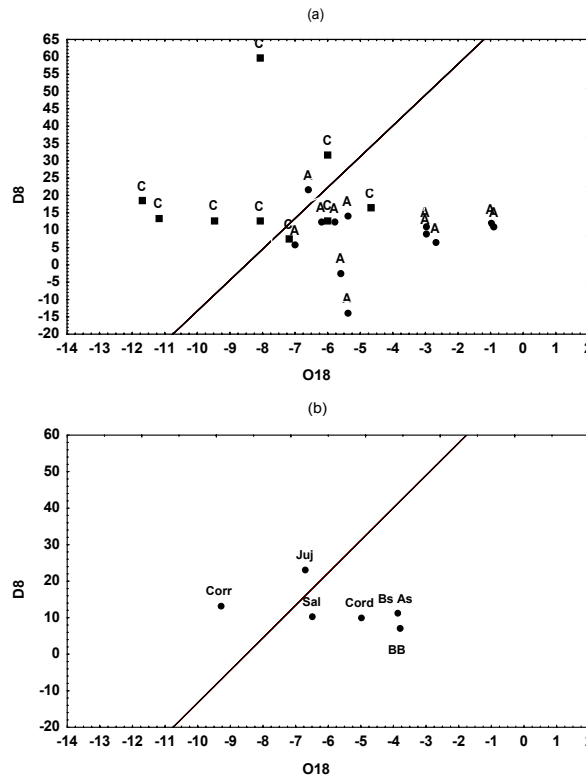


Figure 3: Dispersion diagram of isotopic content (O18 and d8). (a) Cases classified by source. A: Atlantic; C: tropical continental and the corresponding discriminant line. (b) Mean O18 and d8 values for different locations in January.

To discuss the probable origin of water vapor, the mean d8 and O18 values measured at each of the stations are presented for January in figure 3b. These values, both in O18 and in d8, are the result of averaging all the available January samples. Although in summer, the mean low-level flow suggests a continental origin for the air entering

SSA, east of the Andes (Fig. 1c) this does not guarantee a long continental trajectory of the meteoric water. Actually, only Corrientes presents a very likely continental origin (Fig. 3b). In the other stations, the mean values indicate a probable origin from both sources, with more contribution from the Atlantic Ocean in Buenos Aires and Bahia Blanca, the southernmost stations. This indicates that most of the water that precipitates in these areas during January, comes from transient components of the moisture flow. These components, with a trajectory from the Atlantic, may also contribute to the precipitation in the Northwest of Argentina (Salta and Jujuy) and Córdoba (Fig. 3b).

The results from the isotopic contents are consistent with the fields associated to the positive and negative factor loading of the first mode of the integrated water vapor transport (Fig. 2a and 2b). These fields represent cases associated with enhanced and diminished SACZ. When the SACZ is intensified by the flow from the tropical continent, precipitation over southern Brazil, northeastern Argentina and most of Uruguay is depressed by the compensatory subsidence (Nogués-Paegle and Mo 1997; Gandú and Silva Días 1998) (Fig. 2b). For this reason, in spite of the easterly moisture flow that predominates under these circumstances, the meteoric water in Corrientes (northeastern Argentina) shows isotopic contents that are far from the characteristic contents of an Atlantic origin. In addition, Corrientes is in the core of the main low-level transport from the tropical continent of the positive composite (Fig. 2a). The subsidence effect due to the SACZ diminishes further south and west in subtropical Argentina (Fig. 2b), which is consistent with the increased O18 in the rest of the stations. In the case of Bahia Blanca and Buenos Aires, the isotopic contents show an even higher probability that the meteoric waters should originate in the Atlantic rather than in the continent.

3.3 Discussion

Two patterns dominate the water vapor transport variability during midsummer. In the first pattern, the water vapor transport is channeled in a southeastward direction towards eastern SA, south of 20°S, providing moisture convergence for heavy rainfall. As seen from the isotopic contents, the

core of this region in northeastern Argentina receives most of the meteoric water from the tropical continent. On the other hand, this pattern is associated with a weak SACZ

In the other pattern, the tropical water vapor transport is directed towards the SACZ, and consequently, this system is enhanced as it can be inferred from the precipitation field. South of 20°S, there is a westward transport from the Atlantic Ocean that follows an anticyclonic circulation. The subsidence produced by the SACZ, presumably linked to the low-level anticyclonic circulation inhibits precipitation over eastern Argentina, southern Brazil and Uruguay. However, further west and south, the water vapor transport from the Atlantic Ocean favors precipitation, so much that in some locations the isotopic content of meteoric water indicates a prevalence of Atlantic Ocean origin. In the next section, it will be seen that these two patterns are basically reproduced at monthly scale under extreme SST anomalies in the neighboring South Atlantic Ocean.

4. THE LINK BETWEEN SST, SACZ, LOW-LEVEL CIRCULATION AND PRECIPITATION SOUTH OF 20°S

4.1 SST in western subtropical South Atlantic (WSSA)

Doyle and Barros (2002) explored the relationship between interannual western South Atlantic SST north of 40°S and precipitation over eastern SSA using a canonical correlation analysis (CCA). They carried out the CCA using January monthly means as representative of midsummer conditions. The second mode of the CCA has the greatest signal in the precipitation field. The precipitation correlation pattern presents a dipolar structure with opposite and significant values in eastern subtropical Argentina, Uruguay and southern Brazil on the one hand, and in eastern Brazil north of 20°S on the other. The SST second canonical mode shows correlations of the same sign over practically the whole region, with significant values over a large area near the coast, centered at about 23°S, approximately at the mean position of the SACZ. These correlation patterns indicate that precipitation above the mean in the southern dipole center tends to be associated with positive SST anomalies in the WSSA. The northern

center, located at about 500 Km north of the region of the continental extension of the SACZ, presents the inverse behavior, with a tendency to diminished precipitation when warm SST anomalies prevail. If the CCA is performed for the three-month period corresponding to the austral summer, namely December - February, patterns in SST and in precipitation similar to the second mode of the January CCA appear in the first mode (Doyle and Barros 2000). These results are consistent with an earlier work by Díaz et al. (1998) with precipitation over Uruguay and southern Brazil.

In order to analyze further the link between extreme SST, precipitation and low-level circulation, field composites were constructed. The two composites correspond to the warmest and coldest January SST averaged in the region of the greatest SST correlation with the mode of greater precipitation signal, namely, the area within 20°S - 30°S and 30°W - 50°W. The cases in which the SST over this region is higher (lower) than its mean plus (minus) its interannual standard deviation were considered the warmest (coldest) cases. The mean SST in January averaged over this region is 25.3°C, with an interannual standard deviation of 0.5°C. According to this definition, the warmest cases were 1963, 1971, 1973, 1984 and 1988, whereas the coldest ones were 1964, 1965, 1970 and 1985. Hereinafter, they will be referred to as the W and the C cases.

January mean anomalies of skin surface temperature, taken from the NCEP/NCAR reanalyses for W and C composites are shown in figure 4. This is a derived quantity and it depends on the assimilation system. However, figure 4 results basically unchanged in the large-scale features if instead of the skin surface temperature, SST is used. In the case of the continent, there are only some small changes when air surface temperature is used as can be appreciated by comparison of figures 4 and 9. Although the W minus C composite presents the greatest difference in the region where SST was used to define W and C compositions (Fig. 4c), the W and C anomalies are not exactly anti symmetric (Figs. 4a and 4b). In the W composite, the strongest signal over the ocean is displaced to the northeast, while in the C composite it appears to the south with respect to the strongest signal in the W minus C difference. It is interesting to notice that at the latitude of the respective greatest anomalies, the pattern over land

is different. In the W composite, anomalies are positive, as they are over the ocean, while the C

case presents opposite signs over the ocean and land.

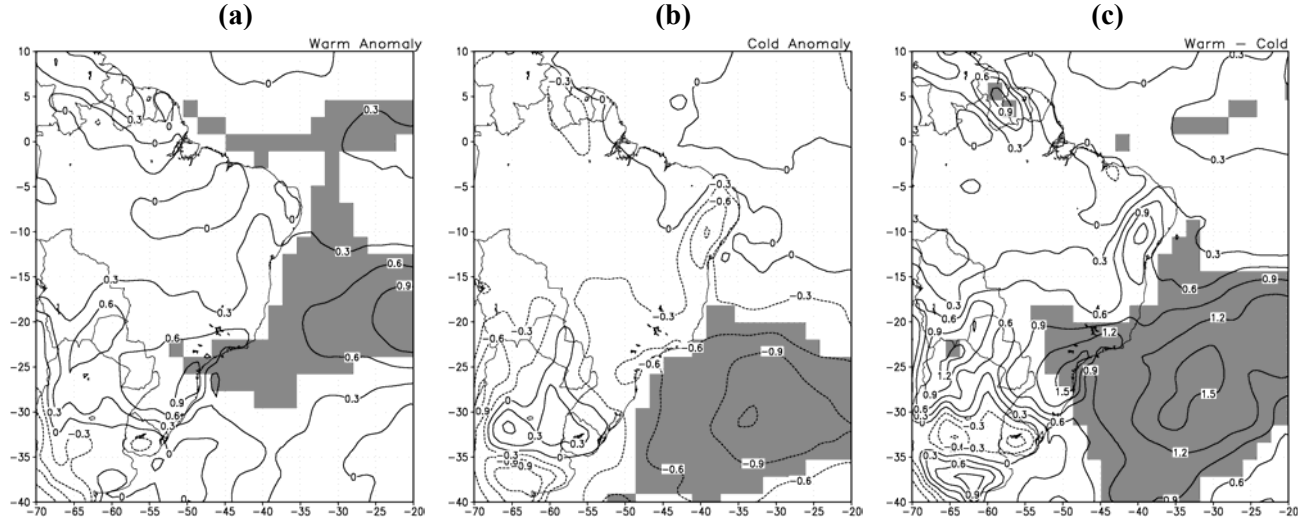


Figure 4: January skin surface temperature (a) W composite (b) C composite and (c) difference between W and C composites (meaning of W and C in the text). Shaded area indicates significant values at 95 % level.

The region with the coldest SST anomalies in the C composite is basically the same as the one taken by Barros et al. (2000) to correlate its average SST with SACZ latitude and intensity. Figure 5 indicates that warm (cold) SST in that region is probably accompanied with a southward (northward) shift of the SACZ. In addition, Barros et al. (2000) showed that the latitudinal shift of the SACZ and its intensity are not independent, since there is a tendency of the SACZ to be weak when displaced southward, and strong when shifted northward. These features will also be seen in section 4.3 when precipitation composites will be discussed.

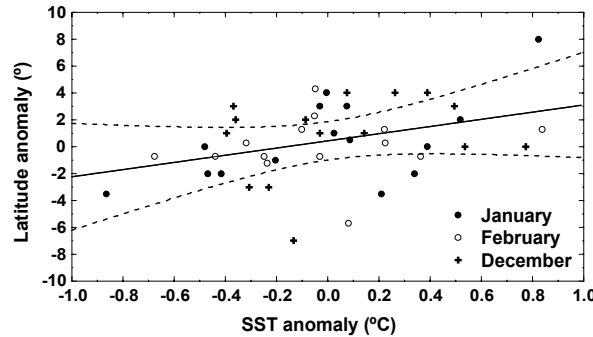


Figure 5: SACZ latitude anomaly vs. Area-averaged SST anomaly. See text for the SST area of averaging.

4.2 Low-level circulation and SST in WSSA

The W and C composites of the 925 hPa wind vector were constructed following the criterion discussed above, and they are presented in figure 6. The W (C) pattern is practically the same as the pattern of the daily positive (negative) composite of water vapor transport (Figs. 2 and 6). Two reasons account for the fact that the patterns of the cases associated with the positive (negative) pattern of the first PCA mode are almost reproduced by the mean low-level circulation corresponding to months with the warmest (coldest) SST in the WSSA. The first is that the low-level wind field determines the integrated low-level water vapor transport because the specific humidity has relatively small spatial variability at the tropical and subtropical latitudes. The second is the prevalence of each of these patterns during the W and C months. In fact, the mean values of the loading factors are 0.2 during the W months and -0.2 during the C months. This indicates that the W and C patterns result, in each case, from the prevalence of one or the other of the two phases of the intraseasonal variability (Doyle and Barros 2002).

The description of the water vapor transport corresponding to the positive composite (Fig. 2) holds for the W composite. Furthermore, in the W

composite, the east–west gradient of geopotential across the eastern continent, between 15°S and 25°S, is consistent with the intense southeastward flow (Doyle and Barros 2002) indicating a deepening of the Chaco low.

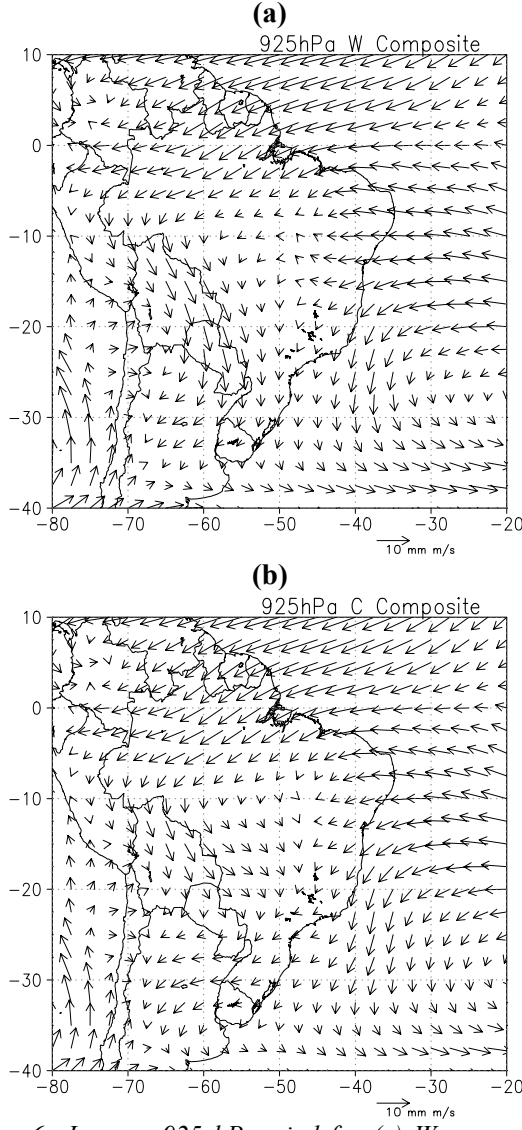


Figure 6: January 925 hPa wind for (a) W composite and (b) C composite.

The C composite pattern has some difference with the negative composite, as the flow from the Atlantic over eastern Brazil has a southward component converging with the eastward branch in the SACZ. In this case, as anticipated in section 3.1, the wind blows from the ocean along the coast of southern Brazil and Uruguay. This flow probably has an additional forcing of a sea–land breeze type, as the land-sea surface temperature gradient attains large values because of the effect

of midsummer conditions in the continent and the coldest anomalies in the ocean (Fig. 4b). The C low-level circulation is so frequent in summer that the average circulation in January shares part of these features (Fig. 1c).

Except over the subtropical continent east of the Andes, the low-level circulation in both the W and C composites is almost identical, which could indicate that differences between both cases in this region might be caused by a regional forcing or by regional processes remotely forced.

4.3 Precipitation and SST in WSSA

The difference in the mean vertical motion (ω) at 500 hPa between the W and C composites is shown in figure 7. With the exception of the SACZ and of the eastern SSA, there are almost no differences in the omega fields corresponding to the W and C cases. A dipole structure between the SACZ and eastern SSA is evident, which is consistent with the pattern observed in the precipitation field (Fig. 8) and with the convergence of the low-level flow (Fig. 6). This structure indicates enhanced activity in the SACZ during the C events, with compensatory subsidence to the south. The opposite behavior is observed in the W composite when the activity over the SACZ area decreases. These features are consistent with results from numerical experiments (Gandú and Silva Días 1998) showing that a strong SACZ is associated with enhanced subsidence south of the SACZ.

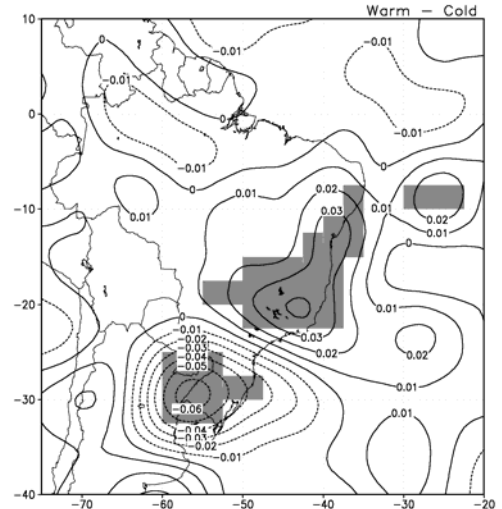


Figure 7: Composite difference of daily 500 hPa ω vertical velocities between W and C January months. Significant values at 95% level are shaded.

January composite precipitation fields corresponding to the W and C cases, as well as their difference, are presented in figure 8. There are two areas of maximum rainfall in the W composite.

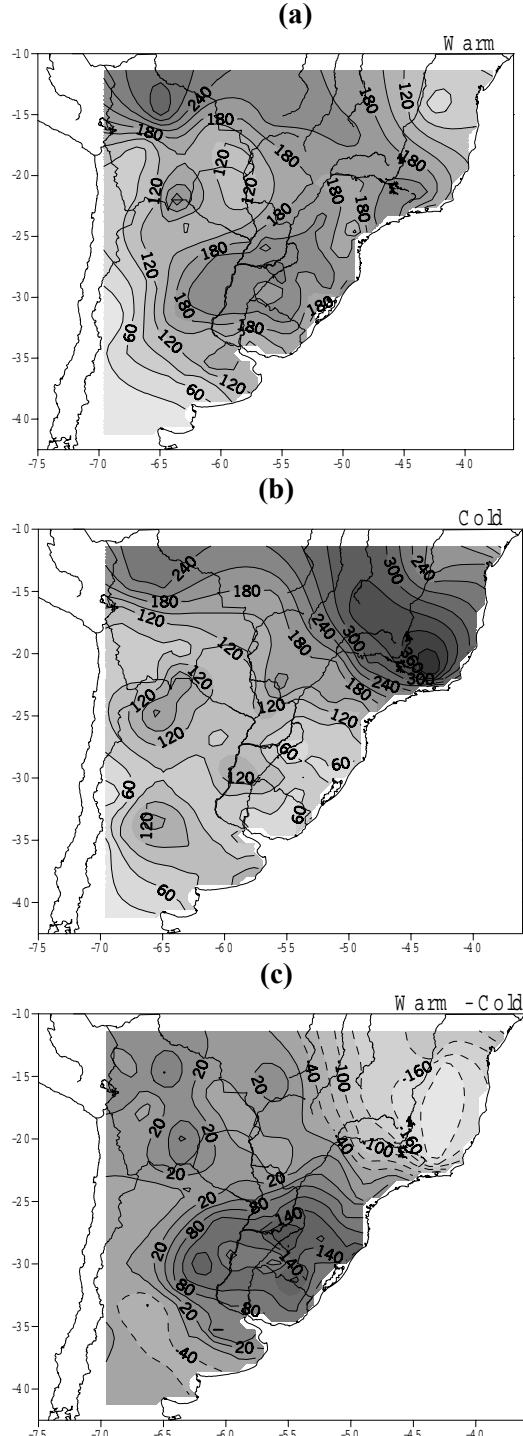


Figure 8: January precipitation for (a) W composite, (b) C composite and (c) difference between W and C cases. Differences greater than 100 mm and below -100 mm are significant at a 95% level.

One has a northwest-southeast direction and encompasses an elongated area with an axis shifted a few hundred kilometers to the southwest of the axis of the mean continental extension of the SACZ. The other maximum, with more than 200mm of monthly rainfall, is centered at about 30°S and 55°W, over part of northeastern Argentina and southern Brazil. The C composite has only a single maximum, elongated in the same way as the first maximum of the W composite, but about 200 Km to the north. The extension of the SACZ over the continent is clearly recognizable in both composites. The precipitation field associated to the SACZ shares its interannual variability (Barros et al. 2000), being more intense (weaker) and shifted to the north (south) in the C (W) composite.

The difference field (Fig. 8c) depicts a dipole structure significant at the 95% level, with centers along the eastern part of the continent: one to the north of the region of the mean continental extension of the SACZ, and the other at about 30°S. The precipitation and the omega vertical velocity difference dipoles, besides being significant in each case, are also consistent with each other in magnitude and location. Since the data of these two fields come from different sources, their consistency adds confidence on the robustness of the signal. Precipitation variability in western and southern subtropical Argentina presents the same sign as the region of the continental extension of the SACZ, although the W minus C values are not significant (Fig. 8c). This could be attributed to the relatively small number of cases analyzed, which is not enough to cope with the large rainfall variability proper of these arid and semiarid regions.

4.4 Continental surface temperature and SST in WSSA

A closer look of the January surface temperature composites over southern SA than that presented in figure 4 is presented in figure 9. In this case the composites were done with surface air temperature taken from the NCEP/NCAR reanalysis. It is worth to mention that regional analyses based on monthly averages using this data set produce essentially similar results as with observed records in SSA (Barros et al. 2002).

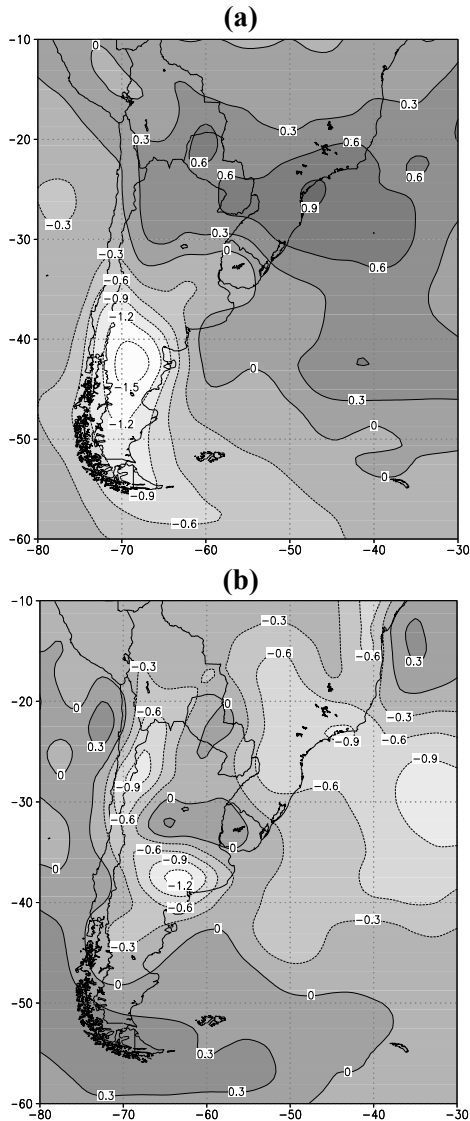


Figure 9: January surface temperature (a) W composite (b) C composite

The W composite (Fig. 9a) has positive surface temperature anomalies north of 30°S consistent with the northern wind (Fig. 6a) that predominates practically throughout the region, except in part of Brazil where the wind blows from the ocean; but in this case, this ocean has positive SST anomalies. The greater positive anomalies are just over the area of a relative minimum in precipitation, located between the two centers of maximum rainfall in southeastern SA (Fig. 8a). To the north of this area, and more clearly to the south of it, the cloudiness associated to maximum rainfall, as well as the increased evaporation, contributes to reduce the effect of the warm horizontal advection. In fact, the interannual correlation between monthly rainfall

and the northern component of the low-level winds is positive throughout most of the year (Barros et al. 2002). As a result, since both processes lead to opposite effects on the surface temperature, there is some sort of compensation resulting in a relatively small interannual variability in surface temperature in SSA east of the Andes (Barros et al. 2002).

Salio et al. (2002) commented that most of the CJEs are associated to a strong contrast between the tropical and the polar air masses. Since the W composite of the low-level flow is characteristic of this type of events, their result is consistent with the more remarkable features of figure 9, that is the strong negative anomaly over Patagonia. It is also an indication of a dominant extratropical low-level circulation associated to the W case.

The C composite (Fig. 9b) shows negative temperature anomalies in the region of the SACZ, in western Argentina along the Andes foothills, and in the southwest of subtropical Argentina. The areas of these negative anomalies correspond well with the areas of enhanced precipitation (see figures 1c and 8b). Although in the case of the western Argentina, the rainfall anomalies are small in absolute value, they might produce an important effect on temperature due to the reduction of the high solar radiation proper of summertime and of the predominant dry conditions in these areas.

4.5 Discussion

As in the case of the low-level circulation, there is a good similarity between the W (C) precipitation fields and the positive (negative) field of daily composites over SSA (Fig. 2 and Figs. 6 and 8). Perhaps the similarity is not even greater because of the different sources for precipitation data (observed data in the case of the W and C composites and, and data from reanalysis in the other case). Thus, the discussion of the relation between the SACZ, the low-level circulation and the precipitation field presented in Section 3.3 holds also for the W and C composites, with the additional concept that each of the two main daily patterns prevails at monthly scale according to the SST field in the WSSA.

SST anomalies in the WSSA could be forced by the low-level atmospheric circulation over eastern SSA, or vice-versa. The similar scale of some SST anomalies and of atmospheric waves, and the correlation between low-level atmospheric cyclonic

circulation and cold SST anomalies, could be considered an indication that large-scale atmospheric waves may cause large SST anomalies (Kalnay et al. 1986). Venegas et al. (1997) applied singular value decomposition (SVD) to coupled fields of surface pressure and SST. They found that in the first mode, where the pressure field roughly represents the variability of intensity of the South Atlantic high, surface pressure usually leads the SST by 1-2 months, indicating an atmosphere-to-ocean forcing. However, in their second mode, which is related to the east-west displacement of the South Atlantic high, the SST leads the surface pressure, revealing an ocean-to-atmosphere forcing, and thus indicating a more complex relationship than a simple one-way forcing. In support of this later view, figure 4 indicates that in the cases with the coldest SST anomalies, the greater anomaly is south of the SACZ. Thus, it is likely that the anticyclonic circulation be enhanced in the southwestern part of the South Atlantic high, thus increasing the eastern component of the low-level flow. In addition, cold SST in the WSSA during midsummer is the most favorable condition for the land-sea temperature gradient to enhance the easterly low-level flow. The meridional component of the pressure gradient resulting from the easterly flow will tend to block the southeastward flow from the tropical continent to the SSA, and consequently, this flow is diverted towards the SACZ, contributing to enhance the SACZ activity.

On the other hand, in view of the remote forcing of the SACZ by Rossby wave propagation (Kalnay et al. 1986; Kiladis and Weickmann 1992; Grimm and Silva Días 1995; Nogués-Paegle and Mo 1997; Liebmann et al. 1999; Lenters and Cook 1999), it cannot be concluded that the low-level circulation patterns in eastern SSA associated with extreme SST anomalies in the WSSA are forced exclusively by these SST anomalies. A more detailed description of these arguments and of a proposed feedback mechanism can be found in Doyle and Barros (2002).

5. LINKS BETWEEN THE ONSET AND END DATE OF THE SAMS AND PRECIPITATION SOUTH OF 20°S

Given the links between the tropical atmosphere and the subtropical climate, it is conceivable that

the variability of the onset and end date of the tropical convection over SA would affect the mean precipitation of the months corresponding to these dates in SSA. A first indication of this point is that tropical convection over SA and precipitation in northwestern Argentina present an almost identical mean annual cycle. González and Barros (1998) calculated the PCAs of the mean annual cycle of both the tropical OLR and precipitation in subtropical Argentina. In each case, the second eigenvectors had a quasi-first harmonic behavior, capturing the annual cycle of each variable. The second OLR PC presented a dipole structure with opposite centers in Central America and Central Brazil, while the second subtropical rainfall PC had the maximum variability in Northwestern Argentina. The second eigenvectors were highly correlated (0.93), indicating quantitatively the almost coincident seasonal variability of both fields. This simultaneous timing can be attributed to the common influence from the annual cycle of the solar heating (Prohaska 1976), or else to an additional physical and direct link between the precipitation processes of these regions.

5.1 Onset and end definition

In tropical and subtropical regions, when OLR is less than a threshold, it is usually indicative of deep convection. This threshold is about 230 to 240 W/m². Thus, Kousky (1988) defined the onset date as the first 5-day average (pentad) when OLR falls below 240 W/m², and satisfies the criterion that OLR in 10 out of the 12 preceding (and subsequent) pentads is above (below) 240 W/m². He also defined the end date as the first pentad when OLR is greater than 240 W/m² and the OLR in 10 out of the 12 preceding (and subsequent) pentads is below (above) 240 W/m². The criteria, involving the preceding and subsequent pentads, preclude the definition of dates by isolated events, while still permitting to seize the trends within the season. It is clear that with these definitions, or other similar definitions based on OLR or precipitation, the onset and demise dates will depend on the threshold chosen. In addition, over tropical SA these dates have a considerable spatial variability (Marengo et al. 2001). The intention here is to treat the onset and the end of convection as an overall large-scale feature of the SAMS. Thus, the onset and end dates calculated for each

grid point in the 2.5° latitude-longitude array, following the criteria employed by Kousky (1988), were averaged in the area between the equator and 15°S , and 45°W and 75°W . However, the extreme northwest of this area, west of 60°W and north of 5°S was excluded, because in some years it was impossible in that region to meet the requirements to determine the onset or the end date. These averages will be hereinafter referred to as the onset and end dates. The averaging area was chosen because it has the swiftest displacement of convection, both during the beginning and the end of the SASM and because it has the greatest OLR seasonal variability in South America south of the equator (González and Barros, 1998).

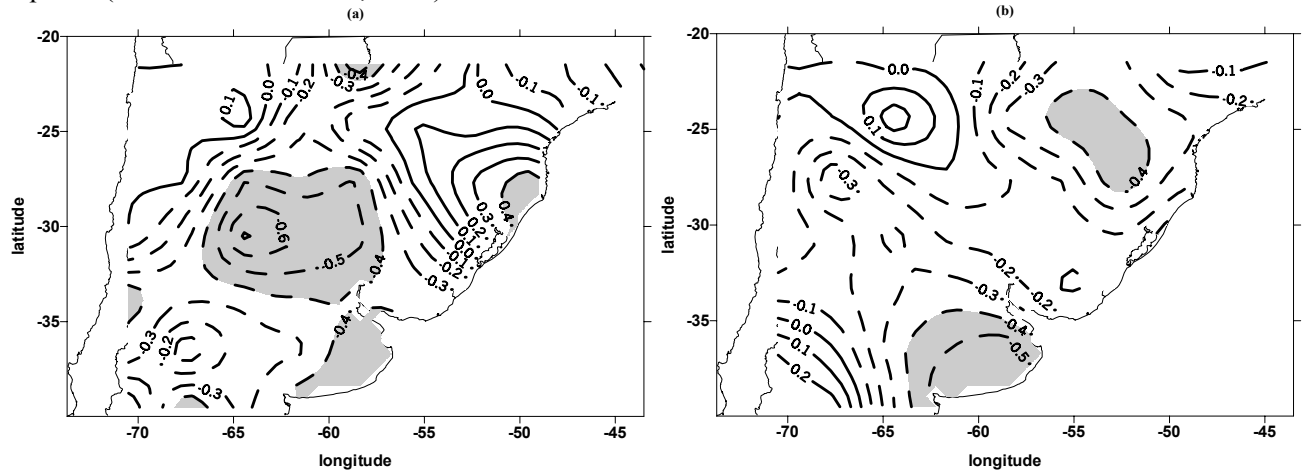
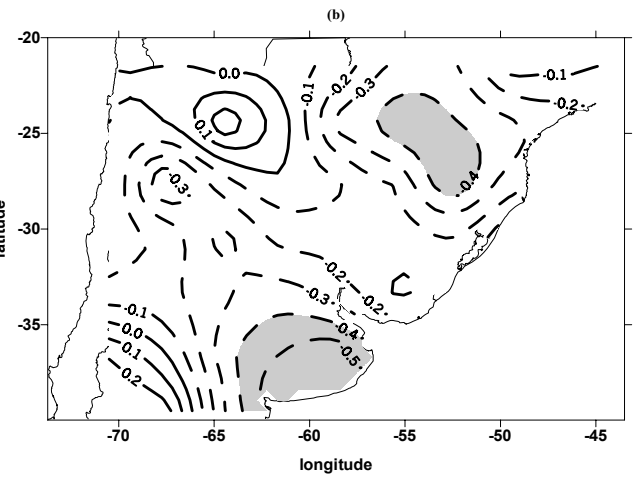


Figure 10: Interannual correlation between (a) the onset date and September rainfall and (b) between the end date and May rainfall for the period 1975-1997. Significant values at a 95% level are shaded.

Figure 11 illustrates the typical evolution of the OLR field during the onset period, presenting a sequence of OLR composite fields corresponding to years with early onsets. Considering the value of 240 watts/m² or less as indicative of convection, figure 11 makes possible to see how the convection propagates very fast from northeastern SA towards the southeast. Moreover, convection near the area of the SACZ develops simultaneously with the progress from the northeast. After some advances and retreats, both areas of convection merge, and only later does convection propagate towards the west near the Andes and to northeastern Brazil. This sequence is basically similar in delayed or early onsets, except for the dates (González and Barros 2002), and it is also insinuated in the mean monthly OLR field of the early spring (Fig. 12). Kousky (1988) also observed this feature in the annual cycle of the mean convection based on pentads. As a consequence of the early

5.2 The onset of the tropical convection and precipitation south of 20°S

The mean onset date for the period 1975-1997 is 23rd September, with a standard deviation of 11 days reflecting an important interannual variability. Figure 10a shows the interannual correlation between September rainfall and the onset date of the tropical convection. The percentage of the area with significant correlation only suffices to claim that it is not attributable to chance with a 20% probability of being wrong (González et al. 2002). However this pattern has a physical meaning, as will be discussed in the next paragraphs.



development of the SACZ and of the compensatory subsidence to the south, the onset date is positively correlated with September precipitation in most of southern Brazil, indicating that the sooner the convection starts, the lower the monthly precipitation is in that area (Fig. 10a).

In the rest of the region, and particularly in central Argentina, the onset date is negatively correlated with September precipitation. This is related to the link between the onset date and the low-level moisture transport from the tropical continent towards the subtropics. González et al. (2002) showed that during early (delayed) onsets, this transport is considerably decreased (increased) towards Eastern Paraguay and Southern Brazil, while on the other hand, there is also a change in the direction of the moisture flow with an increment (reduction) over most of Argentina and Uruguay. This seems to reflect the fact that the

onset accompanies the seasonal change of the low-level flows from winter to spring.

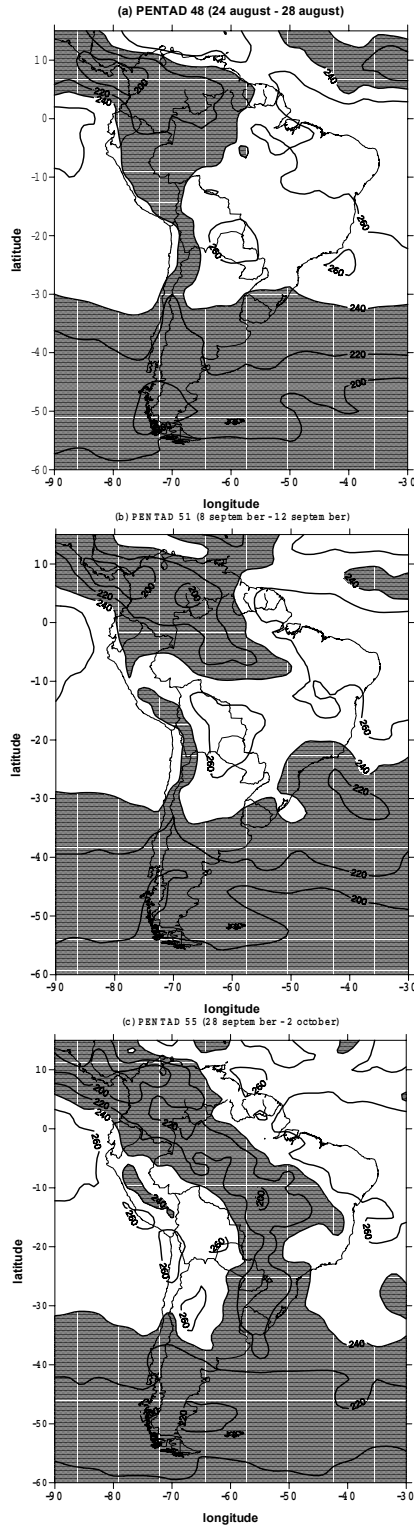


Figure 11: Sequence of OLR composite fields (pentad 48, 51 and 55) corresponding to years with early onsets. Areas with OLR lower than 240 watts/m² shaded.

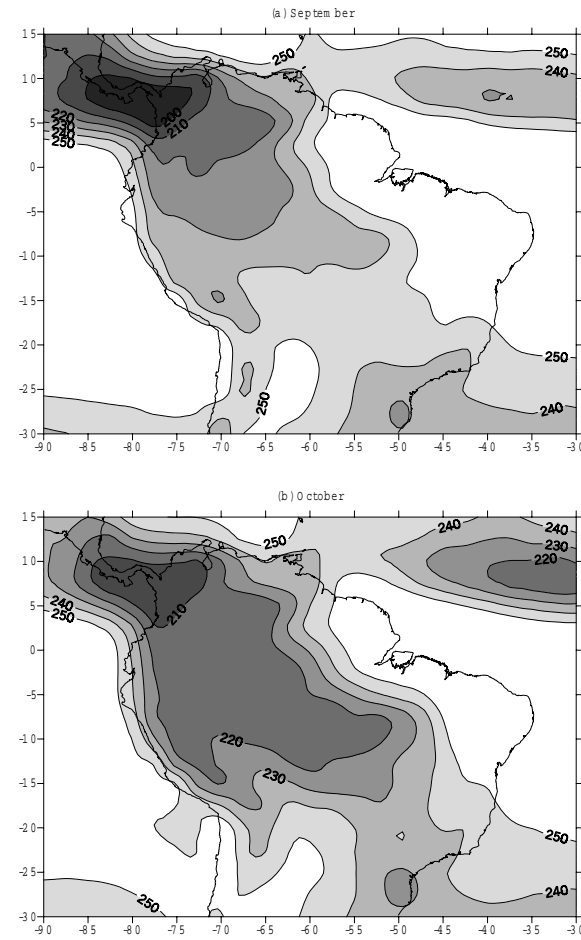


Figure 12: Mean OLR for the period 1975-1999 in (a) September and (b) October.

While in winter the spatial maximum of the flow from the north is over eastern SSA, in spring this maximum flow is located considerably further to the west (Figs. 1a and 1c)

5.3 The end of the tropical convection and precipitation south of 20°S

The end of the convective season over the Amazon region can be considered the last stage in the withdrawal of the SAMS from the Southern Hemisphere. The mean end date is May 14th with a standard deviation of 9 days. This variability may influence the precipitation during May, just like the onset variability does in September.

The interannual correlation between the end date and the precipitation of May is negative over the subtropical region south of 20°S east of the Andes, except in a small area in the northwest of Argentina (Fig. 10b). This implies that when the end takes place earlier (later) than normal, rainfall

tends to be greater (lower) than normal, especially in the two centers with significant negative correlation in southern Brazil and in Buenos Aires Province. There is not an anti-symmetric behavior with respect to the onset correlation field in Argentina; this fact is being addressed hereafter. The area with significant correlation is only a small fraction of the analyzed region, and it is not possible to reject the hypothesis that these significant correlations may occur by chance (González et al. 2002). However, as in the case of the onset, the correlation field has a physical meaning, as it will be shown below.

The CCA first mode of the intra-seasonal variability between OLR north of 20°S and precipitation to the south of this latitude in autumn (pentad data) has a remarkable continuity through this boundary, an indication of the close correlation between the two variables in SSA (Fig. 13). Areas with local significance at the 10% level are large. The probability that this happens by chance is less than 10% (González et al. 2002). There is an association of greater (lower) convection in the northeastern part of the tropical region with lower (greater) than normal rainfall and convection over most of SSA. This dipole pattern resembles the alternating pattern of the SACZ discussed in section 3 for the austral summer. The difference is that in summer, the main center of variability is the northern center at the SACZ (Barros et al. 2000). On the other hand, in the first mode of the autumn, the main center is the southern center, roughly at the location of the maximum of the climatological rainfall (Fig. 1d). The monthly mean OLR fields of the early autumn, namely April and May, show that the demise of the convection starts in the east of SA and progresses with an important westward component (Fig. 14). This implies that, according to the correlation field (Fig. 13), as the convection decreases in the east of Brazil north of 15°S , precipitation to the south of 20°S has a tendency to increase. This is consistent with most of the correlation pattern north of 30°S (Fig. 10b), that indicates that early (delayed) end of the convection is associated to greater (lower) precipitation than normal in this subtropical region.

The mechanism described in the former paragraph does not explain the correlation field south of 30°S . However, González et al. (2002) showed that during early (delayed) end, there is an increased (decreased) low-level moisture transport

from the tropical continent towards the eastern subtropical region. Early and delayed end cases have a difference in the moisture flow towards Southern Brazil, Uruguay and Eastern Argentina whose magnitude is considerable when compared with its mean values. This difference indicates also a more pronounced anticyclonic circulation over the continent, reaching lower latitudes (about 10°S) in the early end cases than in the delayed ones. Therefore, the negative correlation between rainfall in most of SSA and the end date of the tropical convection (Fig. 10b) seems to be determined by the variability of the low-level moisture transport from the tropical continent.

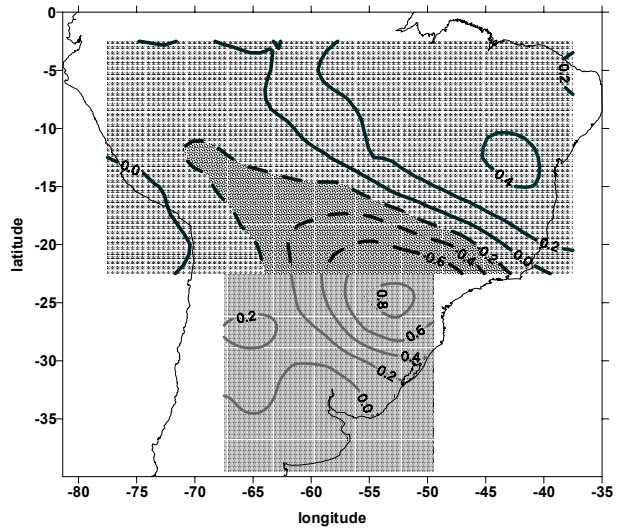


Figure 13: First mode of the canonical correlation between OLR and rainfall for autumn (AMJ) 1975-1997. Significant values at 90% level are shaded.

It can be concluded that the interannual variability of the SAMS's end is associated to the variability in the low-level advection of moisture and precipitation over most of the eastern SSA. Apparently, this link comes from the variability of the progress of the South Atlantic high over the tropical continent in its shift towards lower latitudes during the autumn, which conditions the low-level moisture flow. However, some contribution to this association could come also from a feedback mechanism between rainfall in SSA and convection in tropical SA. In fact, a one-month lagged composite analysis showed that the 500 hPa ω variability in April over southern Brazil, northeastern Argentina and eastern Paraguay is related to the monsoon end date (González and Barros 2002). It is not clear if this is a cause effect

because in April the SST interannual variability is also related to this date, in particular in the case of the tropical Pacific at El Niño regions 1, 2 and 3 and also because that region presents a great El Niño anomaly signal especially during autumn (+) (Grimm et al. 2000; Camilloni and Barros 2000).

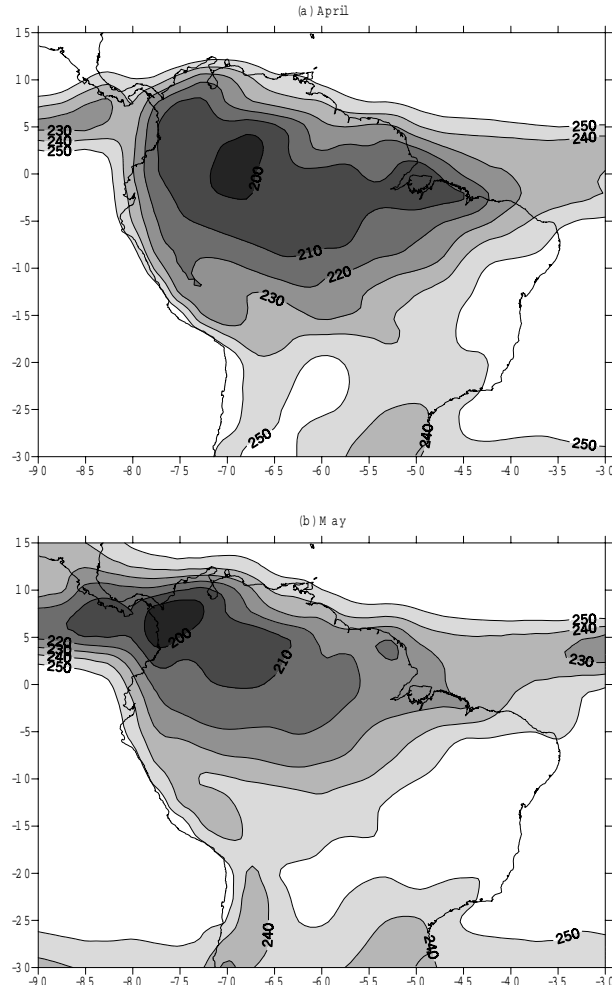


Figure 14: As in Figure 12 but for (a) April and (b) May.

6. IMPACT OF THE SAMS IN THE HYDROLOGY OF THE LA PLATA BASIN

Most of eastern SSA, about $3.2 \times 10^6 \text{ km}^2$, constitutes the La Plata basin (Fig. 15). The two main tributaries of the La Plata estuary are by far, the Paraná and Uruguay rivers. In turn, the Paraná has an important tributary, the Paraguay River. The relation of the SAMS with precipitation south of 20°S conditions some features of the hydrology of these rivers, such as the annual cycle and the

greatest discharges. In this section, the main interest will be on the extreme discharges.

6.1 Floods in the Uruguay River

Compared with the Paraná and Paraguay basins, the Uruguay River basin is relatively small, extending over an area of less than $0.4 \times 10^6 \text{ km}^2$. Because of its size, its narrow transverse section and the steep terrain, the lag between the river discharge and rainfall takes few days (Tossini 1959). According to the Direction of Hydrology of Uruguay, the ten-meter-height of the river in Salto is considered the evacuation mark. We will refer here to the 18 events with the highest mark since the beginning of the record in 1950. These events surpassed the 14 m height and are representative of the largest discharges in the lower basin of the river. Most of them persisted for only a week or less, with the exception of two events, in 1983 and 1998, that were part of flood waves of approximately 2 months duration, both occurring during the strongest El Niño (EN) events of the century. This time scale indicates that the main discharges are usually caused by synoptic events or by a short succession of them. Inspection of each of these events showed that all of them occurred after a few days of a dominant low-level circulation, rather similar to what we call here the positive case (Fig. 2a), which is also the circulation associated with the CJEs (Nicolini and Saulo 2000).



Figure 15: Río de la Plata basin. Rivers and gauging stations in the Paraná and Uruguay Rivers named in the text.

The composite of the low-level circulation of the 12 days before the peak is presented in figure 16. In the four days before the peak (Fig. 16c), the average flow from the northwest over Bolivia and Paraguay converges with a weak component from the north over the Uruguay basin. This circulation pattern is even more intense 12 to 9 days before the peak (Fig. 16a) while 8 to 5 days before (Fig. 16b) the flow from the tropical region is further west.

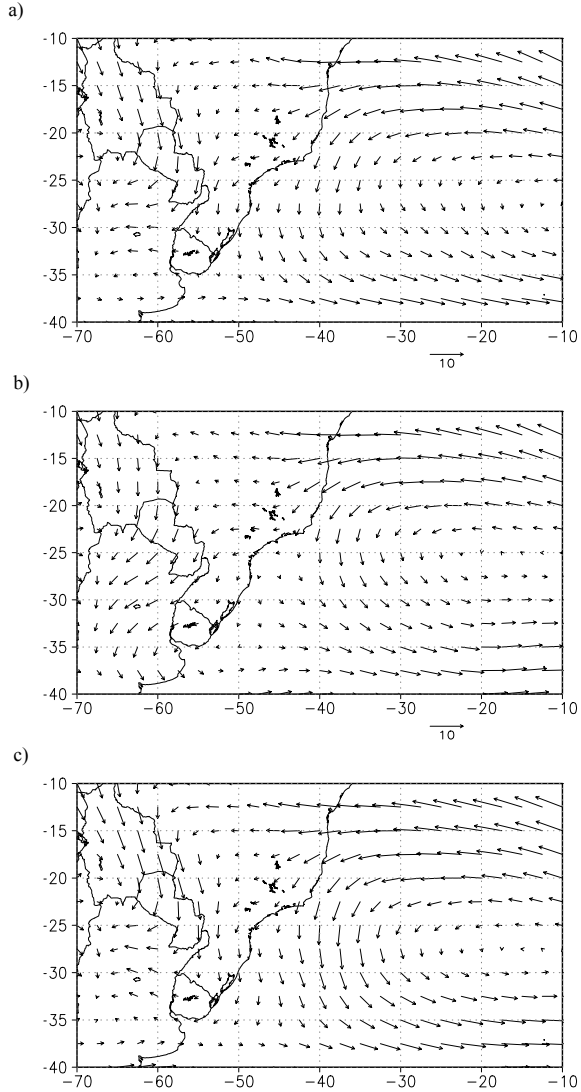


Figure 16: Winds at the 925-hPa composites of three 4-day periods. (a) Composites for the 4 days previous the peak flood date, (b) as in (a) but for the 8th to 5th days, (c) as in (a) but for the 12th to 9th days.

An interpretation of this sequence is that the largest discharges respond typically to two successive events preceded by a strong warm and humid advection from the north. Between these events, there is an intermediate period, probably caused by

a cold frontal passage, which is followed by a period of a few days with the northern flow initially restored over western Argentina and far from the Uruguay basin. If individual cases are inspected, this is confirmed for the cases occurring during the cold semester (April-September), when the highest discharges are observed (Caffera and Camilloni 2002). In summer, there is a tendency to have the greatest northwesterly flow 12 to 9 days before the discharge peak.

6.2 The largest discharges of the Paraná River

Without considering the Paraguay basin, the Paraná River basin covers about half the area of the La Plata basin. It is usually divided in three sub-basins, the Upper Paraná (upstream of the junction with the Grande River), the Middle Paraná (between the junctions with the Grande and the Paraguay rivers) and the Lower Paraná (downstream from Corrientes) basins (Fig. 15). Most of the Paraná River streamflow comes from the upper and middle courses, having a relatively small contribution in its lower section. The high streamflows in the Middle Paraná cause floods over large areas of the Lower Paraná even without a significant local contribution from this sub-basin. Due to the large size of the Paraná basin, its large discharges and floods persist for months, and they are not caused by single synoptic events.

The largest monthly-averaged discharge anomalies of the twentieth century at Corrientes (the outlet of the Middle Paraná) calculated with respect to the 1931-80 monthly means are shown in table I (Camilloni and Barros 2002). These discharges are considerably larger than any possible impact resulting from water management by the upstream dams. In the top ten peaks, the anomalies more than doubled the mean annual discharge of the river. The table includes a classification of the events according to the season and the phase of El Niño-Southern Oscillation (ENSO), and the contribution of each of the sub-basins to these major discharge events. In the case of the Upper Paraná and the upper Middle Paraná, the discharge anomalies corresponding to the month previous to the event in Corrientes were also included, due to the possibility of a zero to one-month lag in the streamflows between these locations.

The largest contributions to the major discharge anomalies in Corrientes come from the

Table I: Major discharge anomalies (m^3/s) at Corrientes and the corresponding discharge anomalies at the Upper Paraná (Jupiá station) and Paraguay (Puerto Bermejo station) and anomaly contribution to discharges (m^3/s) of the upper Middle, lower Middle and Middle Paraná. Previous month discharge or contribution anomaly is indicated in brackets. (0) and (+) stands for El Niño periods as follows: (0) for the onset year of El Niño and (+) for the following year. N/A means no available data.

Corrientes Date and ENSO phase	Upper Paraná	Upper Middle Paraná contribution	Lower Middle Paraná contribution	Middle Paraná contribution	Paraguay
Jun 1983 Autumn (+)	38335	8505 (5360)	18058 (13331)	6121	24179
Jun 1992 Autumn (+)	26787	470 (2502)	10530 (13301)	11322	21852
Dec 1982 Summer (0)	26131	4380 (2273)	9427 (9528)	7584	17011
Mar 1983 Autumn (+)	24231	8368 (13224)	8756 (3648)	3763	12519
Jun 1905 Autumn (+)	24153	N/A (N/A)	N/A (N/A)	N/A	N/A
May 1998 Autumn (+)	22999	380 (-994)	9421 (16284)	8631	18052
Oct 1998 Spring neutral	21006	794 (-434)	15206 (12250)	970	16176
Oct 1983 Spring neutral	20451	5914 (5359)	6363 (6968)	5980	12343
Jul 1982 Winter (0)	18809	2907 (3664)	9154 (2939)	3566	12720
Feb 1997 Summer neutral	17657	874 (7432)	12817 (-2023)	2204	15021
Sep 1989 Spring neutral	16698	990 (1090)	8509 (4490)	3823	12332
Sep 1990 Spring neutral	16410	869 (710)	7935 (5177)	5658	13593
Jan 1912 Summer (0)	15946	N/A (N/A)	N/A (N/A)	N/A	N/A
Nov 1997 Spring (0)	15595	1072 (309)	9814 (9190)	1619	11433
Jan 1966 Summer (0)	15424	3271 (2376)	2624 (3754)	6504	9128
Sep 1957 Spring (0)	15033	1347 (877)	10331 (8449)	1327	11658
					2022

Middle Paraná. In general, these contributions amounted to about two thirds or more of the discharge anomaly computed in Corrientes, and those of the upper part of the Middle Paraná were greater than those of the lower part of the Middle Paraná. The only cases with important contribution from the Upper Paraná occurred during the extraordinary El Niño 1982-1983, or a few months after its end. The contribution of the Paraguay River to the major discharge anomalies in Corrientes enhances the contribution of the Middle Paraná, although in a relatively low proportion.

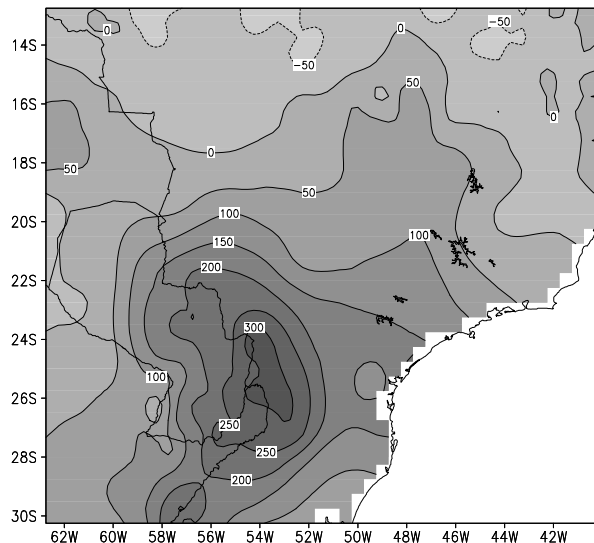


Figure 17: Composite of rainfall anomalies for March (+) to May (+) of El Niño events that persisted until May (+) in El Niño 3 region.

It can be concluded that, with few exceptions, the major discharge events in the Lower Paraná originate in the Middle Paraná basin, more precisely in the upper part of this basin. This basin is in the middle of the dipole structure of precipitation associated to the SACZ activity (Fig. 2) or to the SST in the South Atlantic (Fig. 8). Thus, the major discharges of the Paraná River are not associated to the intensification of any of the phases associated to this dipole; rather, they are associated to other forcings. In fact, according to table I, EN is the most important forcing, although not the only one. The six largest peaks occurred during EN events, and five of them in the autumn of the year following the beginning of the events, autumn (+) (Camilloni and Barros, 2000). As an illustration of this aspect, figure 17 shows the composite of the precipitation anomaly during the

autumn (+) of El Niño events. The magnitude of the anomaly, centered at this basin, almost doubled the mean rainfall in part of the upper Middle Paraná basin (compare with figure 1d).

Although the largest discharges are not related to the midsummer precipitation variability discussed in section 4, its dipole pattern has effect on the Paraná river discharges. In fact, discharge anomalies in January-February of the Upper Paraná, measured at Jupia at 20°S are $-380 \text{ m}^3/\text{s}$ for the W years and $1197 \text{ m}^3/\text{s}$ for the C years, in agreement with the January pattern of variability shown in figure 8. The contribution from the middle Paraná basin to the river discharge offset that of the Upper Paraná as expected according to the precipitation fields (Fig. 8). Thus, the mean discharge anomaly in January - February at Corrientes is $2458 \text{ m}^3/\text{s}$ for the W years and $-2150 \text{ m}^3/\text{s}$ for the C years.

The onset date is not correlated with discharges in September-October of the Paraná, as could be anticipated from the correlation field of this date with the September precipitation (Fig. 10a); there are only weak and non significant correlations with discharges: -0.23 in Jupia and -0.09 in Corrientes. In the case of the end date, there is a significant correlation of -0.51 with Corrientes discharges in May-June. Again this is consistent with the correlation field of precipitation and this date during May (Fig. 10b). Since the signal of figure 10b in southern Brazil and northeastern Argentina is similar to the ENSO signal during autumn (+) (Grimm et al. 2000), it is worth to mention that the correlation of the end date with Corrientes discharge in May-June for no ENSO cases is only slightly different (-0.47) from ENSO years. This indicates that the end date is independent of the ENSO signal on the region.

7. SUMMARY

Figure 18 is a schematic representation of the two main patterns of low-level flow and precipitation anomalies in SSA during midsummer. The prevalence of each of these patterns associated to the seesaw variability of the SACZ varies with the SST in the WSSA. There is a possible positive feedback that might contribute to maintain positive (negative) SST anomalies, weak (intense) SACZ activity, and a W (C) low-level circulation pattern (Doyle and Barros 2002). Thus, the conceptual

diagram of figure 18 is equally valid for the W (C) composites of January means associated to SST anomalies greater (lower) than 0.5°C (-0.5°C) in the area the area within $20^{\circ}\text{S} - 30^{\circ}\text{S}$ and $30^{\circ}\text{W} - 50^{\circ}\text{W}$.

The first pattern (Fig. 18a) includes a main flow from the tropics with a southeastward direction that starting at 10°S converges with the west flow at 35°S over the ocean. In this case, there are positive rainfall anomalies centered in northeastern Argentina and southern Brazil, in the path of the mainstream of the low-level moisture transport. In the second pattern (Fig. 18b), the flow from the tropics turns eastwards towards the SACZ, whereas to the south there is an anticyclonic circulation with

a westward flow over southern Brazil, Paraguay and northern Argentina that turns south when it reaches the Andes Mountains. In this case, rainfall is above its mean values in the continental extension of the SACZ, which is shifted northward of its mean position. Negative anomalies in northeastern Argentina and southern Brazil are a consequence of the compensatory subsidence associated to the more active SACZ and the suppression of the important water vapor transport from the tropical continent. On the other hand, in western Argentina there are positive anomalies in precipitation favored by the transport of moisture from the Atlantic Ocean over this region.

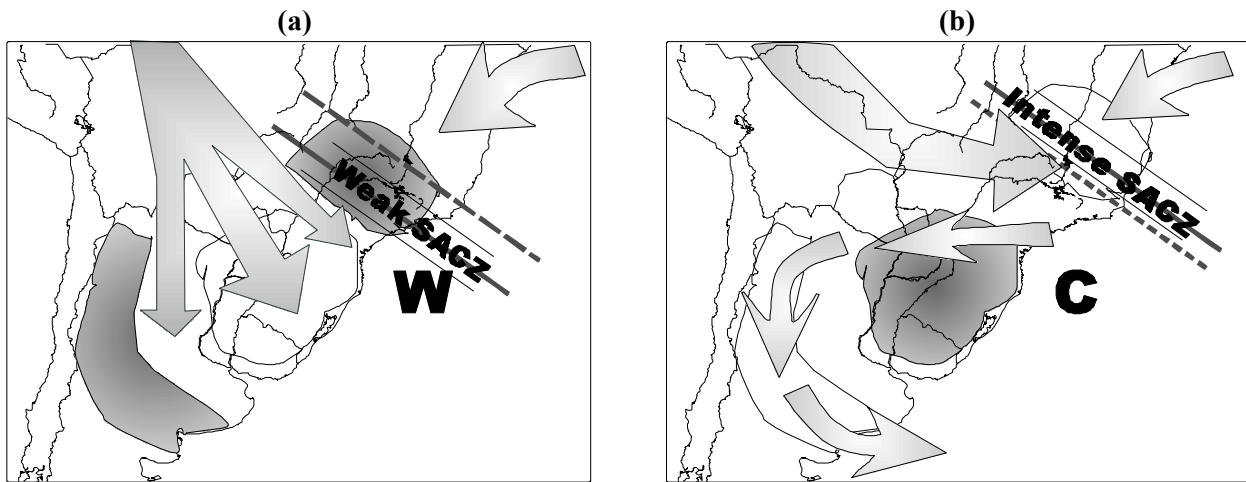


Figure 18: Scheme of the two midsummer dominant patterns of the low-level circulation and of precipitation. Regions with positive (negative) precipitation anomalies are dotted (shaded). Dashed line indicates the approximate mean axis of the convective activity in the SACZ and in its continental extension. W and C stand for similar patterns resulting from SST anomalies as described in the text

The highest discharges in the Uruguay River follow after some days of a low-level circulation of the W type, although they can occur at any time of the year. In the case of the Paraná, the largest discharges are originated in its Middle basin and not during the midsummer. However, as the anomalous precipitation associated to the midsummer variability spreads over part of this basin, it produces a moderate response in the Corrientes discharges.

A delay (an early advent) of the monsoon end increases (reduces) the period with convection over the tropics and the contrary occurs with the onset. Thus, these dates are related with rainfall in SSA east of the Andes during the transition months. In

September, early (delayed) onsets are accompanied with an enhanced (reduced) moisture advection from the tropical continent over most of Argentina and Uruguay, and with a reduction (enhancement) over southern Brazil and Paraguay. This seems to be part of the seasonal trend to the west of the low-level flow from the tropical continent (Fig. 1 a, c). During this month, there is a compensatory subsidence pattern in the vertical velocity field between the tropics and southern Brazil (González et al. 2002); consequently, the onset is positively correlated with rainfall only in southern Brazil while in central Argentina the correlation is highly negative (Fig. 10a)

The interannual variability of the SAMS's end is associated to the variability of the low-level advection of moisture and precipitation over most of eastern SSA. In autumn, the South Atlantic high progresses over the tropical continent in its shift towards lower latitudes. During May, a rapid advance of this system favors both the demise of the convective season and the enhancement of the low-level moisture flow to the subtropics. Thus, the mean low-level flow of moisture over eastern SSA is substantially greater in the cases with advanced monsoon end than in those with a delayed end (González et al. 2002). In addition, as the convection decreases in the east of Brazil north of 15°S, precipitation to the south of 20°S has a tendency to increase (Fig. 13). Consistent with these two aspects, the end date is negatively correlated with rainfall in most of the subtropical region (Fig. 10b).

Acknowledgments. This work was supported by the UBA Project on Floods and the IAI Project CRN-055. The authors are grateful to NOAA-CIRES Climate Diagnostics Center; Boulder, Colorado for permission to include images for figures 11, 12 and 14, calculated from the web site <http://www.cdc.noaa.gov/>.

REFERENCES

- Barros, V., M. González, B. Liebmann and I. Camilloni, 2000: Influence of the South Atlantic convergence zone and South Atlantic sea surface temperature on interannual summer rainfall variability in southeastern South America. *Theor. Appl. Climatol.*, **67**, 123-133.
- Barros, V., A. Grimm and M. Doyle, 2002: Relationship between temperature and circulation in Southeastern South America and its influence from El Niño and La Niña events. *J. Meteorol. Soc. of Japan*, **80**, 21-32.
- Berbery, E. H. and E. M. Rasmusson, 1999: Mississippi moisture budgets on regional scales. *Mon. Wea. Rev.*, **127**, 2654-2673.
- _____ and E. A. Collini, 2000: Springtime precipitation and water vapor flux over southeastern South America. *Mon. Wea. Rev.*, **128**, 1328-1346.
- _____ and V. Barros, 2002: The hydrologic cycle of the La Plata basin in South America. *J. Hydromet.*, **3**, 630 - 645.
- Caffera, R, and I. Camilloni, 2002: Floods over the Uruguay River watershed during 1950-2000: Occurrence and associated atmospheric low level circulation - An approach. PROSUR workshop, 14-16 October 2002. Mar del Plata. On line from http://www-cima.at.fcen.uba.ar/prosur/pr_MdePlataP.htm
- Camilloni, I. and V. Barros, 2000: The Paraná River response to El Niño 1982-83 and 1997-1998 events. *J. Hydromet.*, **1**, 412-430.
- _____ and _____, 2002: The greatest discharge events in the Paraná River and their climate forcing. *J. Hydrology*. (submitted).
- Díaz, A. F., C. D. Strudzinski and C. R. Mechoso, 1998: Relationships between precipitation anomalies in Uruguay and Southern Brazil and sea surface temperature in the Pacific and Atlantic Oceans. *J. Climate*, **11**, 251-271.
- Doyle, M., 2001: Algunos factores que determinan la climatología de la precipitación estival en Argentina subtropical (On some of the factors controlling summer precipitation in subtropical Argentina). Doctoral Dissertation Thesis: University of Buenos Aires, 152 pp.
- _____ and V. Barros, 2000: Relationship between water vapor sources and rainfall over southern South America. *Preprints 6th International Conference on Southern Hemisphere Meteorology and Oceanography*. Santiago de Chile, Chile. AMS. 260-261.
- _____ and _____, 2002: Midsummer low-level circulation and precipitation in subtropical South America and related sea surface temperature anomalies in the South Atlantic. *J. Climate*, **15**, 3394-3410
- Gandú, A. W. and P. L. Silva Días, 1998: Impact of tropical heat sources on the South American

- tropospheric circulation and subsidence. *J. Geoph. Res.*, **103**, d6, 6001-6015.
- González, M. H. and V. Barros, 1998: The relation between tropical convection in South America and the end of the dry period in subtropical Argentina. *Int. J. Climatol.*, **18**, 1669-1685.
- _____, 2002: On the forecast of the Onset and End of the convective season in the Amazon. *Theor. Appl. Climatol.* **73**, 169 -188.
- _____, and M. Doyle, 2002: Relation between the onset and end of the South American summer monsoon and rainfall in subtropical South America. *Climate Research*, **21**, 141-155.
- Grimm, A. M. and P. L. Silva Días, 1995: Analysis of tropical-extratropical interactions with influence functions of a barotropic model. *J. Atmos. Sci.*, **48**, 1822-1836.
- _____, V. Barros and M. Doyle, 2000: Climate variability in southern South America associated with El Niño and La Niña events. *J. Climate*, **13**, 35-58.
- Kalnay, E., K. C. Mo and J. Paegle, 1986: Large amplitude, short-scale stationary Rossby waves in the Southern Hemisphere: Observations and mechanistic experiments to determine their origin. *J. Atmos. Sci.*, **43**, 252-275.
- Kalnay, E., M. Kanamitsu, R. Kistler, W. Collins, D. Deaven, L. Gandin, M. Iredell, S. Sha, G. White, J. Woollen, Y. Zhu, M. Chelliah, W. Ebisuzaki, W. Higgins, J. Janowiak, K. C. Mo, C. Ropelewski, J. Wang, A. Leetmaa, R. Reynolds, R. Jenne, y D. Joseph, 1996: The NCEP/NCAR 40-year Reanalysis Project. *Bull. Amer. Meteor. Soc.*, **77**, 437-471.
- Kiladis, G. N. and M. Weickmann, 1992: Circulation anomalies associated with tropical convection during northern winter. *Mon. Wea. Rev.*, **120**, 1900-1923.
- Kodama, Y. M., 1992: Large-scale common features of subtropical precipitation zones (the Baiu frontal zone, the SPCZ and SACZ) I: Characteristics of subtropical frontal zones. *J. Meteor. Soc. Japan*, **70**, 813-836.
- Kousky, V. E., 1988: Pentad outgoing longwave radiation climatology for the South America sector. *Revista Brasilera de Meteorología*, **3**, 217-231.
- Labraga J., O. Frumento, and M. Lopez, 2000: The atmospheric water vapor cycle in South America and the tropospheric circulation. *J. Climate*, **13**, 1899-1915.
- Laing, A. G., J. M. Fritsch, 2000: The large-scale environments of the global populations of mesoscale convective complexes. *Mon. Wea. Rev.*, **128**, 2756-2776.
- Lenters, J. D. y K. H. Cook, 1999: Summertime precipitation variability over South America: Role of the large-scale circulation. *Mon. Wea. Rev.*, **127**, 409-431.
- Liebmann, B., G. N. Kiladis, J. A. Marengo, T. Ambrizzi, and J. D. Glick, 1999: Submonthly Convective Variability over South America and the South Atlantic Convergence Zone. *J. Climate*, **12**, 1877-1891.
- Marengo, J., 1992: Interannual Variability of surface climate in the Amazon Basin. *Int. J. Climatol.*, **12**, 853-863.
- _____, B. Liebmann, V. Kousky, N. Filizola and I. Wainer, 2001: Onset and end of the rainy season in the Brazilian Amazon basin. *J. Climate*, **14**, 833-852.
- Nicolini, M. and A. C. Saulo, 2000: ETA characterization of the 1997-1998 warm season Chaco jet cases. 6th International Conference on Southern Hemisphere Meteorology and Oceanography, Santiago de Chile, 3-7 April. AMS, 336-337.
- Nogués-Paegle, J. and K. C. Mo, 1997: Alternating wet and dry conditions over South America during summer. *Mon. Wea. Rev.*, **125**, 279-291.
- Paegle, J., 1998: A comparative review of South American low level jets. *Meteorologica*, **23**, 73-81.

Climate variability over Subtropical . . .

- Prohaska, F.J., 1976: Climates of Central and South America. World Survey of Climatology. Elsevier Scientific Publishing Company, Amsterdam, pp. 57-69.
- Randel, D. L., T. H. Vonder Haar, M. A. Ringerud, G. L. Stephens, T. J. Greenwald, and C. L. Combs, 1996: A new global water vapor dataset. *Bull. Amer. Meteor. Soc.*, **77**, 1233-1246.
- Rao, V., I. Cavalcanti and K. Hada, 1996: Annual variation of rainfall over Brazil and water vapor characteristics over South America. *J. Geophys. Res.*, **101**, 26539-26551.
- Rozanski, K., L. Araguas and R. Gonfiantini, 1993: Isotopic patterns in modern global precipitation, Climatic Change in Continental Isotopic Records, *Geophysical Monograph* 78. pp. 36
- Salati, E., L. Molion and J. Marques, 1978: Origen y distribución de las lluvias en el Amazonas (*Origin and distribution of rainfall in Amazon*). *Revista Interciencia*, **3**, 200-205.
- Salio, P., M. Nicolini, and A. C. Saulo, 2002: Chaco low-level jet events characterization during the austral warm season by ERA reanalysis. VAMOS/CLIVAR/WCRP Conference on South American low-level jet. Santa Cruz de la Sierra, Bolivia, 5 - 7 February. (http://www-cima.at/fcen.uba.ar/sallj/SALLJ_Conference_extabs_A43.pdf).
- Schotterer, U., F. Oldfield, and K. Frohlich, 1996: Global Network for Isotopes in precipitation. *Pages*. IAEA, WMO and IAHS, Switzerland. pp. 47.
- Tossini, L., 1959: Sistema hidrográfico y Cuenca del Río de la Plata. Contribución al estudio de su régimen hidrológico. (Hydrographic system and basin of the La Plata River: Contribution to the study of the hydrologic regime). *Anales de la Sociedad Científica Argentina*, Marzo-Abril 1959, III y IV, Tomo CLXVII, 41-64.
- Velasco, I., and J. M. Fritsch, 1987: Mesoscale convective complexes in the Americas. *J. Geophys. Res.*, **92**, D8, 9591-9613.
- Venegas, S. A., L. A. Mysak and D. N. Straub, 1997: Atmosphere-ocean coupled variability in the South Atlantic. *J. Climate*, **10**, 2904-292.
- Vera, C. S., P. K. Vigliarolo, and E. H. Berbery, 2002: Cold season synoptic scale waves over subtropical South America. *Mon. Wea. Rev.*, **130**, 684-699.
- Virji, H., 1981: A preliminary study of summertime tropospheric circulation patterns over South America estimated from cloud winds. *Mon. Wea. Rev.*, **109**, 599-610.
- Woodruff, S. D., R. J. Slutz, R. L. Jenne and P. M. Steurer, 1987: A comprehensive ocean-atmosphere data set. *Bull. Amer. Meteor. Soc.*, **68**, 1239-1250.
- Zhou, J. and K. M. Lau, 1998: Does a monsoon climate exist over South America? *J. Climate*, **11**, 1020-1040